



A COMPARATIVE ANALYSIS OF DIFFERENT COLOR SPACES FOR RECOGNIZING ORANGE FRUITS ON TREE

R. Thendral and A. Suhasini

Department of Computer Science and Engineering, Annamalai University, Chidambaram, Tamil Nadu, India

E-Mail: thendralamutha@gmail.com

ABSTRACT

Segmenting ripe fruits region in the foliage is an important step in agriculture sector applications of yield measurement, robot harvesting, and fruit grading. In this paper, we present a fundamental study of different color spaces RGB, HSV, L*a*b and YIQ with the motivation of analyzing, which color space is convenient for ripe fruits recognition from the background. The results show that 'I' component of the YIQ color space has the best criterion for recognizing the ripe fruits from the other regions.

Keywords: color spaces, ripe fruits, image processing, segmentation.

1. INTRODUCTION

India is an expansive agrarian nation. Agribusiness has given careful consideration since old. Our precursor has created a lot of better approaches to make the marvelous rural human progress. With the advancement of horticulture engineering, farming modernization raises new prerequisites for agribusiness improvement. Then again, previous customary recognition strategies have not fulfilled the prerequisite of up-to-date horticulture, which promotes modern detection technology applied. Around them machine vision technology can give proficient and dependable items recognition approach. Fruits picking by humans is a time-consuming, tiresome and expensive process. Because of this, the automation of fruit harvesting has accomplished great popularity in the last decade. Therefore, image processing and use of automation techniques in agriculture have become a major issue in recent years.

System designs based on automatic image analysis technology that are already getting used in other areas of agriculture [1, 2] including applications in the field. For instance, the system designed for pre-sorting of apples [3], respectively in the field. Further examples of the usage of machine vision technology operation in the fields are those applied to automate the harvesting task. Basic research on robotic harvesting initiated with orchard fruits [4, 5]; after that, this kind of studies have been ongoing in several countries [6]. This technology has then been useful for vegetable fruits. Several prototype robots are reviewed [7] and clarified the importance of the manipulator design and its applications for practical use. Several researchers have applied robotic technology to fields in greenhouses; such as tomatoes [8], oranges [9], melons [10] and cucumbers [11]. A thorough review [12] with regard to fruit recognition system shows, the performance and cost have not satisfied commercial requirements.

Several studies have been carried out to recognize fruits on the tree based on robotic harvesting, such as in orange [13] fruit recognition R/(R+G+B) feature and for cotton [14] recognition R-B feature was used from RGB color modal. Luminance and red color plane difference (R-

Y) was only used for Fuji apple [15] recognition. OHTA color spaces based image segmentation algorithm was used for the robotic strawberry harvesting system [16]. Skin defect detection of apples by L*a*b* color space features [17] and pomegranates by HSI color space features [18] was used.

Recognition of fruit on trees is an important and still challenging issue in agriculture, which has potential applications ranging from fruit load estimation to yield forecasting and robotic harvesting. Automated vision-based recognition of fruit has been studied intensively. In this present study, we compare the twelve different color components for ripe fruits recognition based on histograms of the color components (R, G, B, H, S, V, L*, a*, b*, Y, I, Q). The color component with the best peak histogram is selected in order to recognize the ripe fruits on the tree.

2. MATERIALS AND METHODS

To validate the proposed recognition algorithm, 40 on tree orange fruit images were randomly selected from the internet. These images were then transferred to the computer and all proposed algorithms were developed in the MATLAB environment using image processing toolbox version 7.0.

a) Segmentation

Image segmentation acts as the key of image analysis and pattern recognition. It is a process of dividing an image into different regions such that every single region is uniform, but the union of any two regions is not [19]. A proper definition of image segmentation is as follows: If $P(\cdot)$ is a homogeneity predicate described on groups of connected pixels, then segmentation is a separator of the set F into connected subsets or regions (S_1, S_2, \dots, S_n) such that

$$\bigcup_{i=1}^n S_i = F, \text{ with } S_i \cap S_j = \emptyset, \quad (i \neq j)$$

The uniformity predicate $P(S_i) = \text{true}$ for all regions, S_i and $P(S_i \cup S_j) = \text{false}$, when $(i \neq j)$ and S_i and S_j are neighbours.



Color of an image can have much more information than the gray level. In most pattern recognition and computer vision applications, the additional information provided by color is able to help the image analysis method and also yield better results than approaches using only gray scale information [20]. Most research has focused on color image segmentation due to its demanding needs. At present, color image segmentation methods are mainly extended from monochrome segmentation approaches by being implemented in different color spaces.

Color spaces are different bases for representing intensity and color information in color images. Usually color spaces have three components or channels for representing all possible color and intensity information. Selecting the best color space still is one of the difficulties in color image segmentation for each application. The aim of the segmentation process in this study was to recognize the ripe fruits from the background. For this purpose, we compare the twelve different color spaces and choose the suitable color space in order to separate the ripe fruits from leaves, and tree branches.

b) Primary space

RGB is a very commonly used three-dimensional color space with color components or channels red, green, and blue.

Red, green, and blue elements can be described by the illumination values of the location obtained through three separate filters (red, green, and blue filters) depending on the following equations

$$R = \int_{\lambda} E(\lambda) S_R(\lambda) d\lambda$$

$$G = \int_{\lambda} E(\lambda) S_G(\lambda) d\lambda$$

$$B = \int_{\lambda} E(\lambda) S_B(\lambda) d\lambda$$

Where S_R, S_G, S_B are the colour filters on the incoming light or radiance $E(\lambda)$, and λ is the wavelength. The R, G, B color components of an acquired image is device dependent [21]. Lighting condition of greenhouse was not equal in the time of image acquisition. The RGB color model could not be lonely used to recognize mature fruits because of the high correlation among the R, G, and B components [22, 23]. Figure-1 shows the monochrome images of red, green and blue color channels and it is corresponding one-dimensional histograms.

c) Perceptual space

Human describes colors by hue, saturation, and brightness. Hue (H) and saturation (S) define chrominance, while intensity or value (V) specifies luminance. The HSV color space [24] is defined as follows

$$H = \begin{cases} \theta, & \text{if } B \leq G \\ 360 - \theta, & \text{if } B > G \end{cases}$$

$$\text{Where } \theta = \cos^{-1} \left\{ \frac{\frac{1}{2} [(R-G) + (R-B)]}{[(R-G)^2 + (R-B)(G-B)]^{\frac{1}{2}}} \right\}$$

$$S = 1 - \frac{3}{R+G+B} [\min(R, G, B)]$$

$$V = \frac{1}{3}(R+G+B)$$

HSV is computed from a nonlinear transformation of RGB color space and normalized to a range of 0 to 255. This is consistent with the histogram representation in intensity with the values from 0 to 255. Figure-2 shows the monochrome images of hue, saturation and value color channels and it is corresponding one-dimensional histograms.

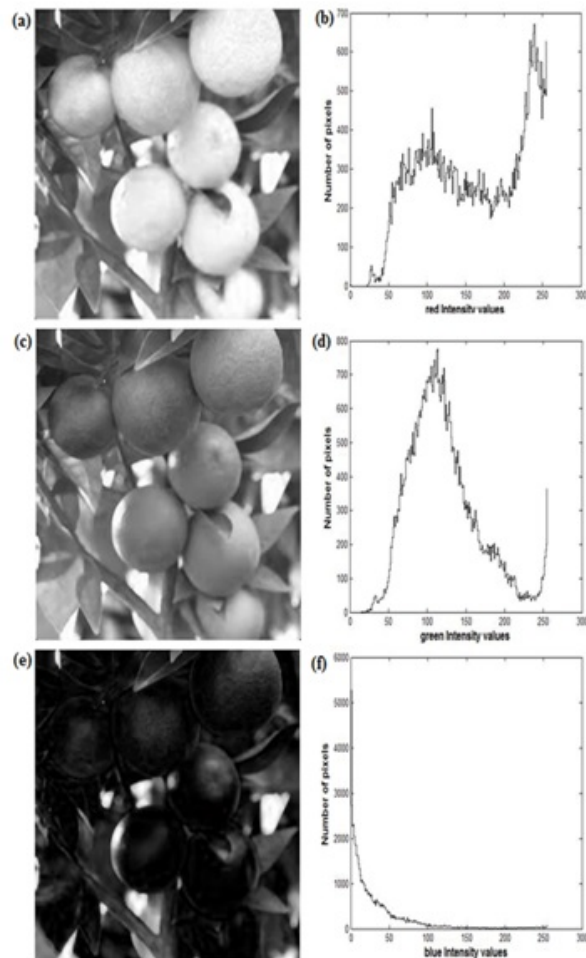


Figure-1.(a) & (b) red color component and its corresponding histogram plot analysis; (c) & (d) blue color component and its corresponding histogram plot analysis;



(e) & (f) green color component and its corresponding histogram plot analysis.

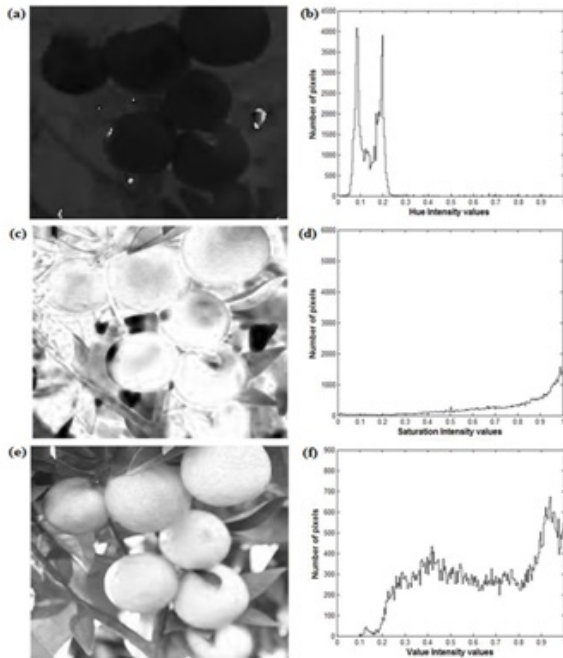


Figure-2. (a) & (b) hue color component and its corresponding histogram plot analysis; (c) & (d) saturation color component and its corresponding histogram plot analysis; (e) & (f) value color component and its corresponding histogram plot analysis.

d) Luminance-chrominance spaces

1) CIE $L^*a^*b^*$: The Commission International de l'Eclairage (CIE) color system defines three primary colors, denoted as X, Y, and Z. XYZ coordinates originate [25] from a linear transformation of RGB space, as indicated by

$$\begin{bmatrix} X \\ Y \\ Z \end{bmatrix} = \begin{bmatrix} 0.607 & 0.174 & 0.200 \\ 0.299 & 0.587 & 0.114 \\ 0.000 & 0.066 & 1.116 \end{bmatrix} \begin{bmatrix} R \\ G \\ B \end{bmatrix}$$

CIE $L^*a^*b^*$ seems to have more uniform perceptual properties than another CIE space, CIE $L^*a^*b^*$. It is obtained through a nonlinear transformation on XYZ.

$$L^* = 116 \left(\sqrt[3]{\frac{Y}{Y_0}} \right) - 16$$

$$a^* = 500 \left[\left(\sqrt[3]{\frac{X}{X_0}} \right) - \left(\sqrt[3]{\frac{Y}{Y_0}} \right) \right]$$

Where (X_0, Y_0, Z_0) are the XYZ values for the standard white. The 'L' component in the $L^*a^*b^*$ color space corresponds to lightness ranging from 0 (black) to 100

(white), the 'a' component corresponds to the measurement of redness (positive values) or greenness (negative values), and the 'b' component corresponds to the measurement of yellowness (positive values) or blueness (negative values).

CIE spaces have metric color difference sensitivity to a good approximation and are very convenient to measure the small color difference, while the RGB space does not [26]. Figure-3 shows the monochrome images of L^* , a^* and b^* color channels and it is corresponding one-dimensional histograms.

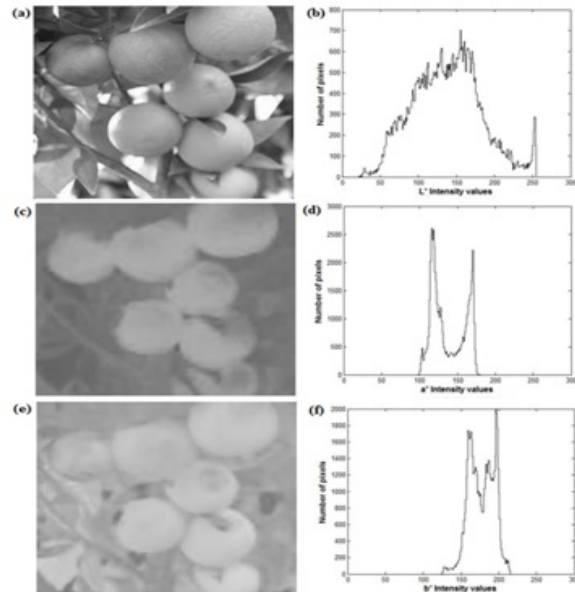


Figure-3. (a) & (b) L^* color component and its corresponding histogram plot analysis; (c) & (d) a^* color component and its corresponding histogram plot analysis; (e) & (f) b^* color component and its corresponding histogram plot analysis.

2) YIQ: The linear transformation of the RGB to YIQ conversion is defined by the following matrix transformation

$$\begin{bmatrix} Y \\ I \\ Q \end{bmatrix} = \begin{bmatrix} 0.299 & 0.587 & 0.114 \\ 0.596 & -0.274 & -0.322 \\ 0.212 & -0.523 & 0.311 \end{bmatrix} \begin{bmatrix} R \\ G \\ B \end{bmatrix}$$

where $0 \leq R \leq 1$, $0 \leq G \leq 1$, $0 \leq B \leq 1$. 'Y' component corresponds to luminance (lightness), and 'I' component corresponds to the orange – cyan axis, and 'Q' component corresponds to the magenta – green axis [27]. The YIQ color model can partly neutralize the interrelation of the red, green and blue components in an image. Figure-4 shows the monochrome images of Y, I and Q color channels and it is corresponding one-dimensional histograms.

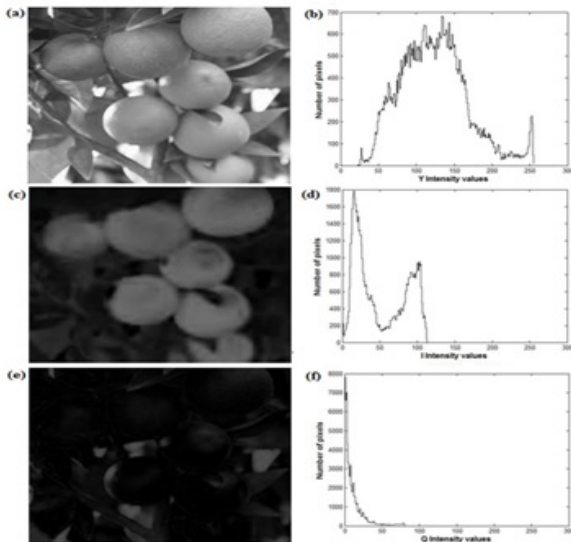


Figure-4. (a) & (b) Y color component and its corresponding histogram plot analysis; (c) & (d) I color component and its corresponding histogram plot analysis; (e) & (f) Q color component and its corresponding histogram plot analysis.

Among all the planes, except in the instance of 'I' component, the fruits and other objects were highly presented in the images. So it was just about difficult to find an appropriate fruit area from the other color spaces. So from the YIQ color space 'I' image plane (see Figure-4(c)) was utilized for the contour detection of fruit regions because this plane was considered as pixels of fruit regions and small amount of canopies. So, this step was used for the contour detection of probable fruit regions within a given input image. The flowchart of the process of ripe fruit recognition can be seen in Figure-5.

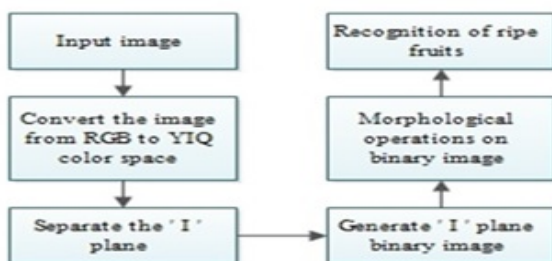


Figure-5. Overview of our recognition method.

3. RESULTS AND DISCUSSIONS

a) Recognition of ripe fruits

Input image transformed into the YIQ color model and separate the 'I' plane to recognize the ripe fruits. The recognized pixels were represented by the value of '1' while the rest of the pixels were represented by the value of '0'. This resulted in the binary representation of the 'I' plane (see Figure-6(a)) in which the fruit areas are represented as white and the background was represented

by black color. Due to the variation in illumination among the image in the Normal-view category and the presence of some dead leaves, certain pixels were falsely classified as fruits. After the binary conversion, the ripe fruits are in the image, but still some objects are available these are not fruits. It was essential to filter out or else reduce this noise. These unwanted parts are eliminated by applying the dilation with an appropriate kernel size and removing the small objects present in the binary image. Resulting image (see Figure-6(b)) contained the recognized ripe fruits only. This binary mask image changed over to the same type of the input image. To remove the background, the binary mask image was multiplied in R, G and B channels separately. The color image was reconstructed by composition of R, G and B channels got from the past step. The resultant image (see Figure-6(c)) shows the recognized fruit regions only.

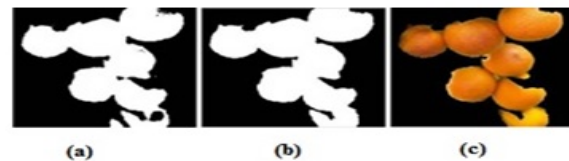


Figure-6. (a) 'I' plane converted into a binary image; (b) Morphological operations resultant image; (c) Extracted resultant fruit regions.

4. CONCLUSIONS

In this paper, a vision algorithm was designed to recognize the ripe fruits from the other objects of image. Recognition algorithm developed in this study used color difference components ('I' channel) as criteria for discriminating the ripe fruits from the leaves and boughs. This algorithm could identify ripe fruits by high accuracy in different lighting conditions of a greenhouse. About 93% area of a ripe fruits was extracted by the proposed algorithm.

REFERENCES

- [1] S. Cubero, N. Aleixos, E. Moltó, J. Gomez Sanchis, and J. Blasco. 2011. Advances in machine vision applications for automatic inspection and quality evaluation of fruits and vegetables. *Food Bioprocess Tech.* Vol. 4, no. 4, pp: 487-504.
- [2] D. Lorente, N. Aleixos, J. Gómez Sanchis, S. Cubero, O. L. Garcia Navarrete, and J. Blasco. 2012. Recent advances and applications of hyperspectral imaging for fruit and vegetable quality assessment. *Food Bioprocess Tech.* Vol. 5, no. 4, pp. 1121-1142.
- [3] A. Mizushima, and R. Lu. 2010. Cost benefits analysis of in-field presorting for the apple industry. *Appl. Eng. Agric.* Vol. 27, no. 1, pp. 22-40.



- [4] C. Schertz. and G. Brown. 1968. Basic considerations in mechanizing citrus harvest. Transactions of the ASAE. Vol. 11, no. 2, pp. 343-348.
- [5] E. Parrish. and A. Goksel. 1977. Pictorial pattern recognition applied to fruit harvesting. Transactions of the ASAE. Vol. 20, no. 5, pp. 822-827.
- [6] Y. Sarig. 1993. Robotics of fruit harvesting: a state-of-the-art review. J. Agr. Eng. Res. Vol. 54, no. 4, pp. 265-280.
- [7] N. D. Tillett. 1993. Robotic manipulators in horticulture a review. J. Agr. Eng. Res., Vol. 55, no. 2, pp. 89-105.
- [8] P. P. Ling, R. Ehsani, K. C. Ting, Y. Chi, N. Ramalingam, M. H. Klingman. and C. Draper. 2004. Sensing and end-effector for a robotic tomato harvester. In Proc. the ASAE/CSAE annual international meeting, Aug. Ottawa, Paper Number: 043088 [CDROM], ISBN 0-929355-94-6, Ontario, Canada. St Joseph, MI: ASAE Publisher.
- [9] G. Muscato, M. Prestifilippo, N. Abbate. and I. Rizzuto. 2005. A prototype of an orange picking robot: past history and experimental results. Vol. 32, no. 2, pp. 128-138.
- [10] Y. Edan, D. Rogozin. T. Flash. and G. E. Miles. 2000. Robotic melon harvesting. IEEE Trans. Robot. Autom. Vol. 16, no. 6, pp. 831-834.
- [11] E. Van Henten, J. Hemming, B. Van Tuijl, J. Kornet, J. Meuleman, J. Bontsema. and E. 2002. Van Os. An autonomous robot for harvesting cucumbers in greenhouses. Auton. Robots, Vol. 13, no. 2, pp. 241-258.
- [12] A. R. Jimenez, R. Ceres. and J. L. Pons. 2000. A survey of computer vision methods for locating fruit on trees. Transactions of the ASAE. Vol. 43, no. 6, pp. 1911-1920.
- [13] M. W. Hanan, T. F. Burks. and D. M. Bulanon. 2009. A machine vision algorithm combining adaptive segmentation and shape analysis for orange fruit detection. Agricultural Engineering International: CIGR Ejournal. Vol. 11, Manuscript 1281.
- [14] Y. Wang, X. Zhu. and C. Ji. 2008. Machine vision based cotton recognition for cotton harvesting robot. Computer and Computing Technologies in Agriculture, pp. 1421-1425.
- [15] D. M. Bulanon, T. Kataoka, Y. Ota. and T. Hiroma. 2002. A Segmentation Algorithm for the Automatic Recognition of Fuji Apples at Harvest. Biosyst. Eng., Vol. 83, no. 4, pp. 405-412.
- [16] F. Guo, Q. Cao. and M. Nagata. 2008. Fruit detachment and classification method for strawberry harvesting robot. International Journal of Advanced Robotic Systems, Vol. 5, no. 1, pp. 41-48.
- [17] G. Moradi, M. Shamsi, M. H. Sedaaghi. and S. Moradi. 2011. Apple defect detection using statistical histogram based fuzzy C-Means algorithm. In 7th Iranian conf. machine vision and image processing, pp. 1-5.
- [18] M. M. Pawar. and M. M. 2012. Deshpande. Skin defect detection of pomegranates using color texture features and DWT. In National Conf. Computing and Communication Systems. pp. 1-5.
- [19] H. D. Cheng, X. H. Jiang, Y. Sun. and J. Wang. 2001. Color image segmentation: Advances and prospects. Pattern Recogn. Vol. 34, no. 12, pp. 2259-2281.
- [20] J. M. Gauch. and C. W. Hsia. 1992. A comparison of three color image segmentation algorithms in four color spaces. In proc. the SPIE Visual Communications Image Processing, Vol. 1818, pp. 1168-1181.
- [21] H. J. Trussell, E. Saber. and M. Vrhel. 2005. Color image processing," IEEE Signal Proc. Mag. Vol. 22, no. 1, pp. 14-22.
- [22] M. Pietikainen. 1996. Accurate color discrimination with classification based on feature distributions. In proc. the 13th Int. Conf. Pattern Recognition. Vol. 3, pp. 833-838.
- [23] E. Littmann. and H. Ritter. 1977. Adaptive color segmentation, a comparison of neural and statistical methods. IEEE Transactions on Neural Networks, Vol. 8, no. 1, pp. 175-185.
- [24] A. R. Smith. 1978. Color gamut transform pairs. Computer Graphics, Vol. 12, no. 3, pp. 12-19,
- [25] J. M. Tenenbaum, T. D. Garvey, S. Wyl, H. C. Wolf. and D. Nitzan. 1974. An interactive facility for scene analysis research. Artificial Intelligence Center, Stanford Research Institute, Menlo Park, California, Technical Note 95.
- [26] G. Robinson. 1977. Color edge detection. Opt. Eng., Vol. 16, no. 5, pp. 479-484.
- [27] W. Che Yen. and C. Chun Ming. 2004. Color Image Models and its Applications to Document Examination," Forensic Science Journal. Vol. 3, no. 1, pp. 23-32.